

Computational Multiscale Mechanics Laboratory (CMML)

Shaoping Xiao, Assistant Professor

**Department of Mechanical and Industrial Engineering
Center for Computer-Aided Design**

The University of Iowa

TEL: 319-335-6009 FAX: 319-335-5669

Email: shaoping-xiao@uiowa.edu

Website: www.engineering.uiowa.edu/~sxiao

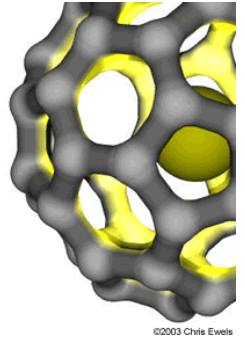
Research assistants:

Weixuan Yang, PhD student

Maciej Rysz, Undergraduate student

Former student:

Wenyi Hou (PhD, Caterpillar)



Nanoscale

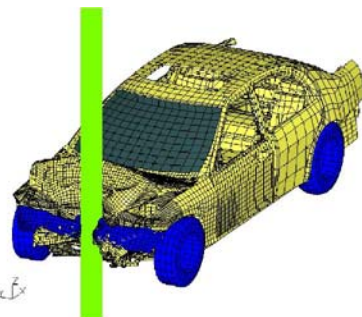


Microscale

Mesoscale



Macroscale



Meshfree particle methods (Macro-scale ~1m)

- Treatment of large deformations and fractures
- Stability Analysis
- A coupling method of meshfree particle method with finite element method

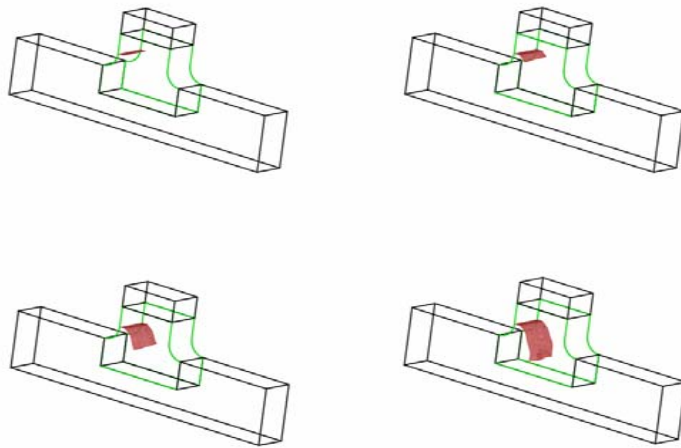


Fig. 2 Meshfree particle method coupled with FEM for 3D crack propagation

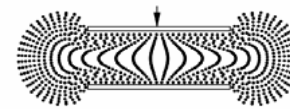
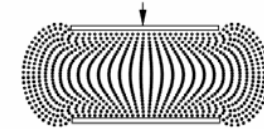
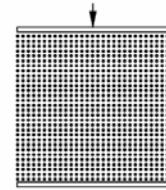
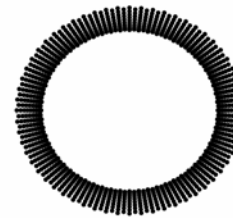
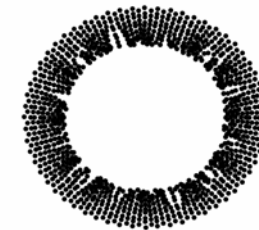


Fig. 1 Meshfree particle methods can sustain large deformations



(a) Lagrangian kernel



(b) Eulerian kernel

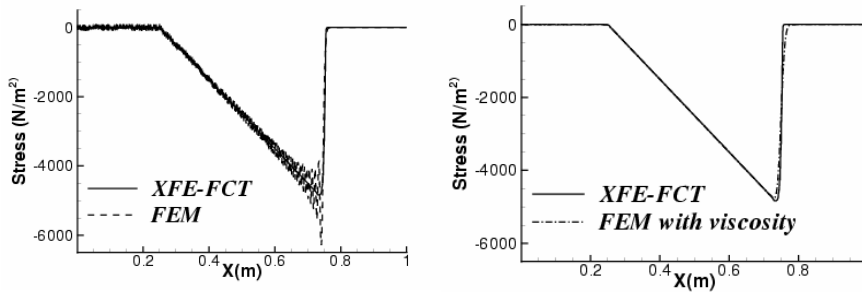
Fig. 3 Rubber ring extension shows that meshfree particle method with Lagrangian kernel (a) is more stable than with Eulerian kernel (b)

- Rabczuk, *et. al.*, *Communications for Numerical Methods in Engineering*, Vol 22(10), 2006, pp 1031-1065
- Xiao and Belytschko, *Advances in Mathematical computation*, Vol 23, 2005, pp 171-190
- Rabczuk, *et. al.*, *Computer Methods in Applied Mechanics and Engineering*, Vol. 193, 2004, pp. 1035-1063
- Belytschko and Xiao, *Computers and Mathematics with Applications*, Vol. 43(3-5), 2002, pp.329-350



FE-FCT method and dynamic fracture (Macro-scale ~1m)

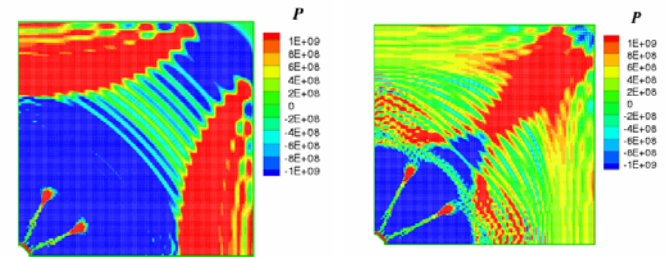
- Treatment of shock wave propagation and interaction as well as dynamic fracture such as spallation
- A total Lagrangian FE method with structured mesh
- An implicit function is used to describe the arbitrary boundaries
- The flux-corrected transport (FCT) algorithm is used to eliminate the oscillations behind shock wave fronts



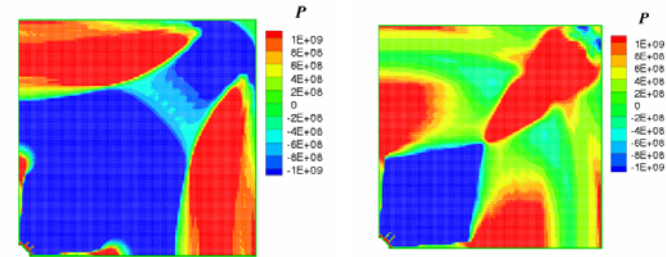
	Theoretical analysis	FE-FCT method	FE with viscosity	FE method
Spall thickness	0.225m	0.226m	0.230m	0.201m

Fig. 4 The FE-FCT method can eliminate the fluctuations as well as keep strong discontinuities. This non-oscillatory method can accurately predict spallation and spall thickness.

- Xiao, *Communications for Numerical Methods in Engineering*, Vol 23, 2007, pp 71-84
- Xiao, *International Journal for Numerical Methods in Engineering*, Vol 66, 2006, pp 364-380
- Xiao, *Wave Motion*, Vol 40, 2004, pp 263-276



(a) FE method



(b) FE-FCT method

Fig. 5 A plate with a central hole with explosion occurring along the circumference of the hole. The fluctuation behind shock wave fronts is observed when performing the conventional FE method. However, the FE-FCT method can eliminate the fluctuation and accurately describe the shock wave propagation and interaction.



Topological optimization (Meso-scale ~1mm):

- Structured extended finite element method
- An implicit function is used to describe the boundary
- The method can describe hole creation and emerging

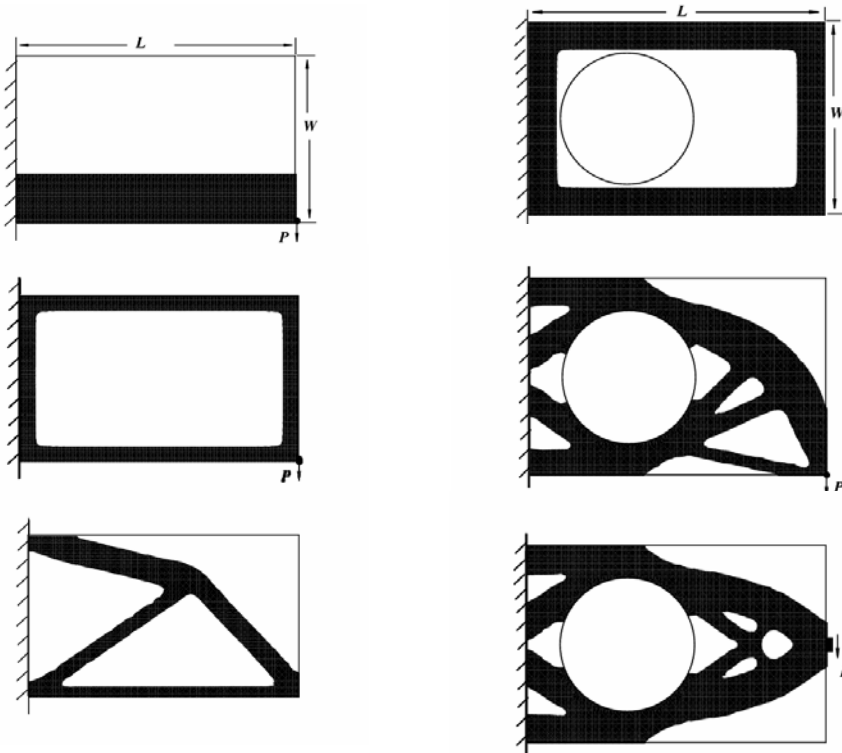


Fig. 6 optimal design can be obtained no matter what initial design is given

Fig. 7 optimal designs of structures contain a hole with different loads

- Belytschko, *et. al.*, *International Journal for Numerical Methods in Engineering*, Vol. 57, 2003, pp.1177-1196

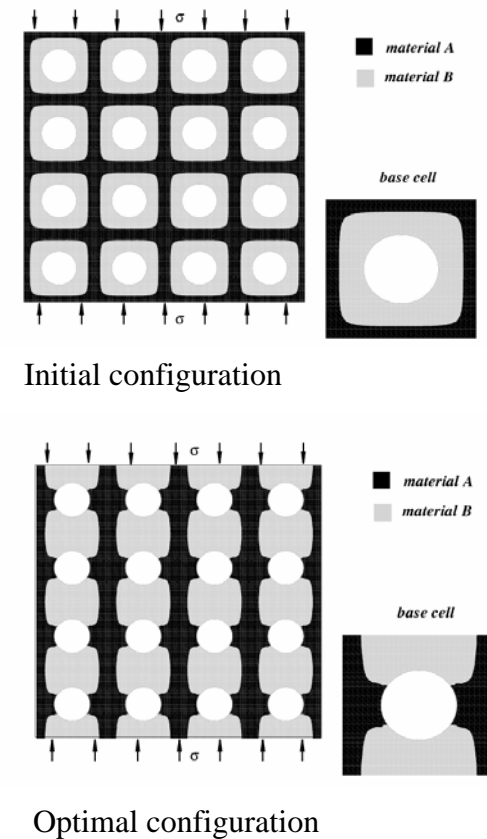


Fig. 8 optimal design of a composite with holes. The simulation is performed on a unit cell



Cell mechanics (Micro-scale $\sim 1\mu\text{m}$)

- Understanding mechanics of cultured endothelial cells in response to PKC activation.
- The tensegrity model ignores the contributions of the cell shell, the cytoplasm and the nucleus .
- A structural model of the filamentous cytoskeleton that integrates and considers additional elements, such as the cell shell, the cytoplasm and the nucleus, is proposed.

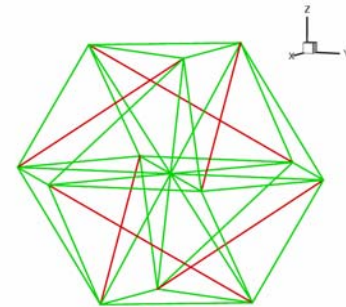


Fig. 9 Tensegrity model of a single cell

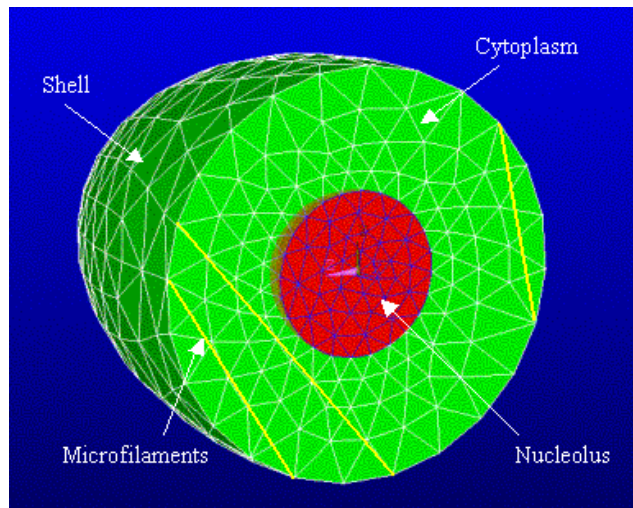


Fig. 10 A finite element model of living cells

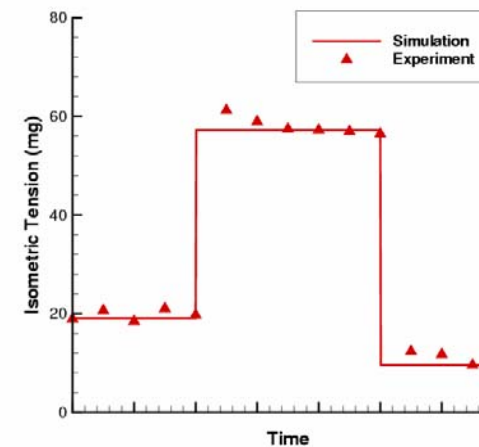


Fig. 11 evolution of isometric tension of a cell sheet in response to thrombin and cytochalasin activation



Temperature-related homogenization (Micro-scale $\sim 1\mu\text{m}$)

- Temperature-related Cauchy-Born (TCB) rule considering the free energy instead of the potential
- Assumptions: 1) atoms have locally homogeneous deformation; 2) atoms have the same local vibration modes; 3) the vibration of an atom is harmonic; and 4) coupled vibration of different atoms is negligible
- Verifications and material stability analysis

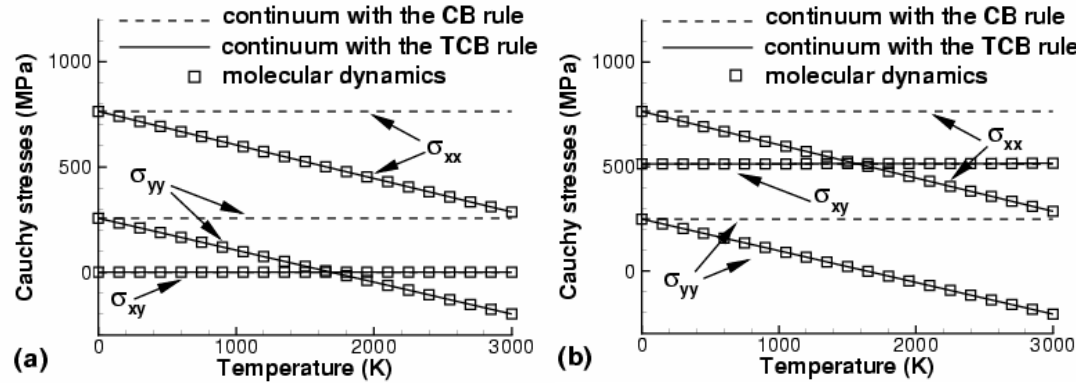


Fig. 12 Comparison of Cauchy stress components at various temperatures in a two-dimensional Lennard-Jones crystal subjected to the following deformation gradients: (a) $F_{11} = 1.001$, $F_{12} = F_{21} = 0.0$, $F_{22} = 1.0$; and (b) $F_{11} = 1.001$, $F_{12} = 0.002$, $F_{21} = 0.0$, $F_{22} = 1.0$

- Xiao and Yang, *International Journal for Numerical Methods in Engineering*, Vol 69, 2007, 2099-2125
- Xiao and Yang, *Computational Materials Science*, Vol 37, 2006, pp 374-379

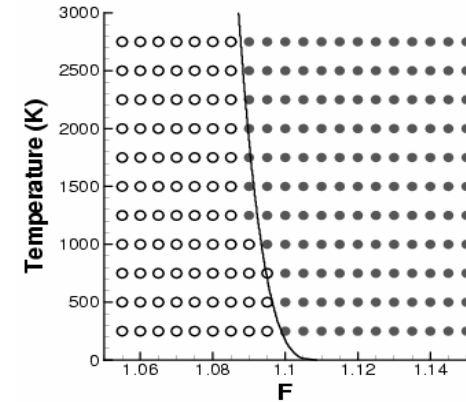


Fig. 13 Stable domain of 1-D molecular chain

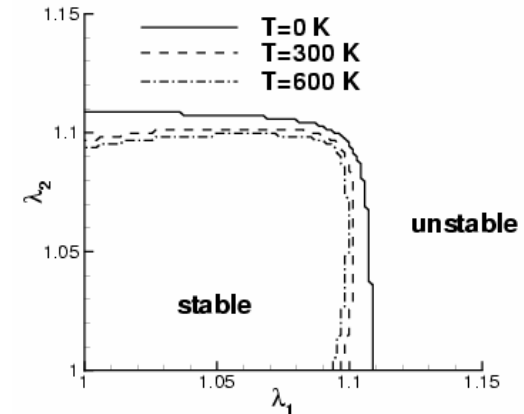


Fig. 14 Stable domain of 2D LJ crystal



A hierarchical multiscale method (Micro/Nano-scales $\sim 1\mu\text{m}-1\text{nm}$)

- The meshfree particle methods with the implementation of a homogenization technique
- A temperature-related Cauchy-Born rule

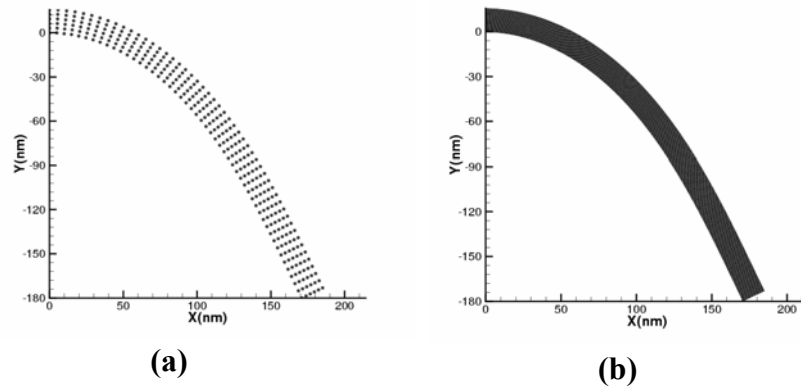


Fig. 15 Bending of a nanobeam. The meshfree particle method result (a) compares well with the molecular mechanics result (b). The comparison of the potential evolution (c) supports the above conclusion

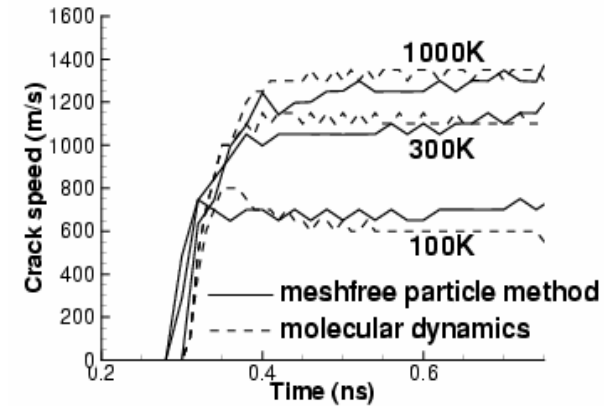
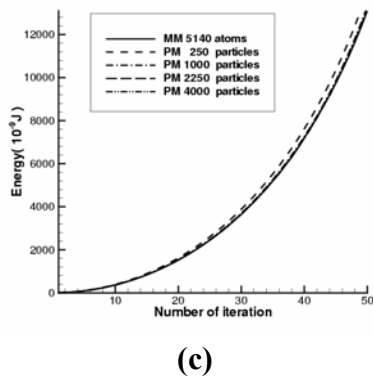


Fig. 16 The calculated temperature-dependent crack speeds are compared well with the results of MD simulations.

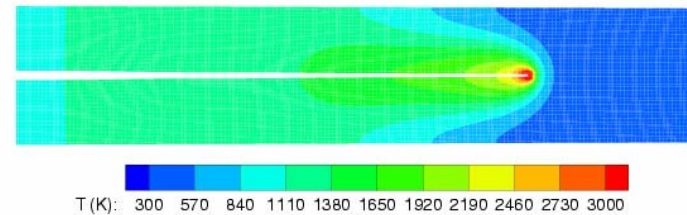


Fig. 17 temperature profile when the crack propagating

- Xiao and Yang, *International Journal for Numerical Methods in Engineering*, Vol 69, 2007, 2099-2125
- Xiao and Yang, *The International Journal of Computational Science and Engineering*, Vol 2(3-4), 2006, 213-220
- Xiao and Yang, *International Journal of Computational Methods*, Vol. 2(3), 2005, pp. 293-313



A concurrent multiscale method (Micro/Nano-scales $\sim 1\mu\text{m}$ -1nm)

- A bridging domain coupling method
- Molecular domains and continuum domains are overlapped via bridging domains
- An explicit algorithm is developed so that the nonphysical spurious reflection phenomena can be avoided.

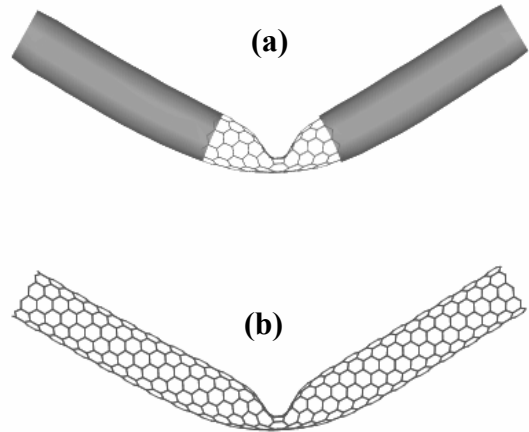


Fig. 18 Bending of a single-walled carbon nanotube: (a) Bridging domain coupling method simulation; (b) molecular mechanics calculation

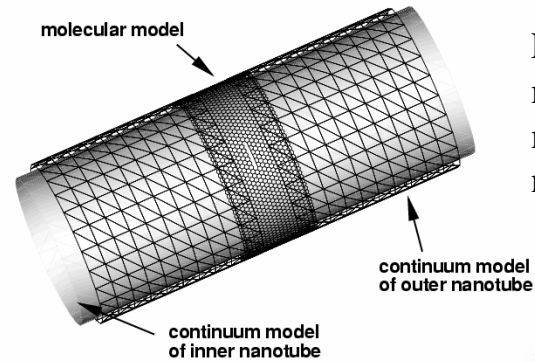


Fig. 19 Bridging domain multiscale modeling for multi-walled carbon nanotube fracture

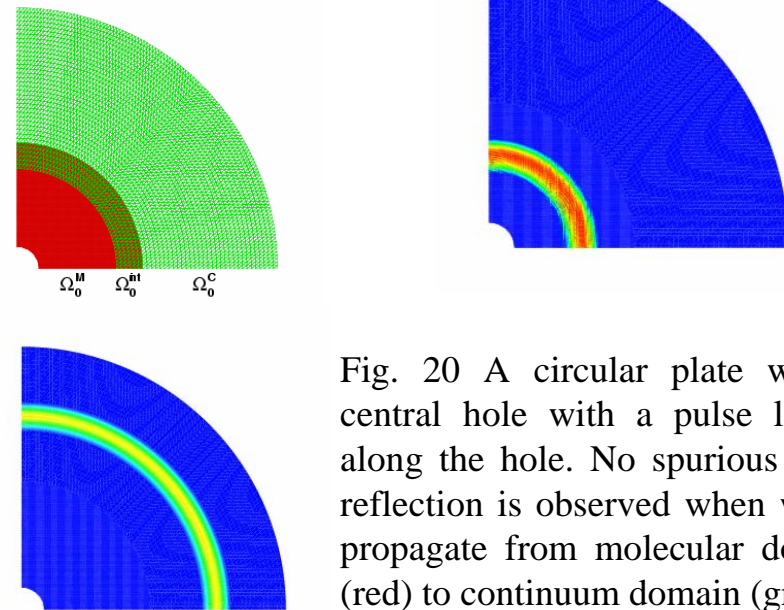


Fig. 20 A circular plate with a central hole with a pulse loaded along the hole. No spurious wave reflection is observed when waves propagate from molecular domain (red) to continuum domain (green)

- Xiao and Belytschko, *Computer Methods in Applied Mechanics and Engineering*, Vol. 193, 2004, pp. 1645-1669
- Belytschko and Xiao, *Journal of Multiscale Computational Engineering*, Vol. 1(1), 2003, pp.115-126



Mechanics of nanotubes (Nano-scale ~1nm)

- Size effects on carbon nanotubes' mechanical properties
- Mechanics of Defect-free and defective carbon nanotubes (CNTs)
- Vacancy defects can dramatically reduce nanotube strength

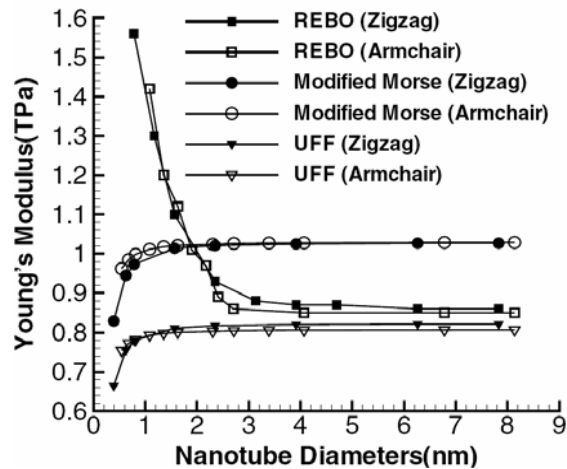


Fig. 21 Studies of size effects on the Young's modulus of a single-walled carbon nanotube. Three potential functions are used in atomistic simulations. The trend confliction is observed for different potential functions.

- Xiao and Hou, *Physical Review B*, Vol 73, 2006, 115406
- Xiao and Hou, *Fullerenes, Nanotubes, and Carbon Nanostructures*, Vol 14, 2006, pp 9-16
- Mielke et. al., *Chemical Physics Letters*, Vol 390, 2004, pp 413-420
- Belytschko et. al., *Physical Review B*, Vol 65, 2002, 235430

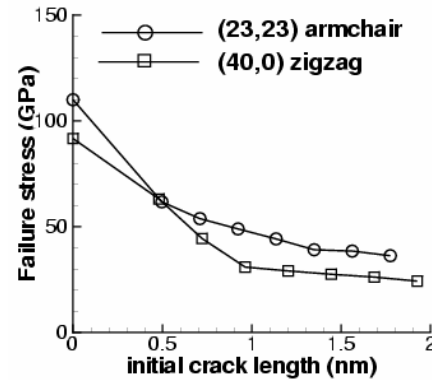
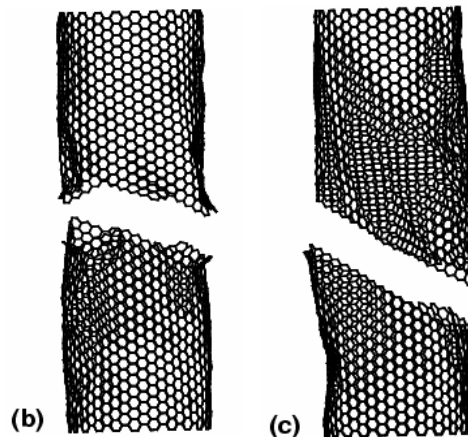


Fig. 22 Failure stresses of defected nanotubes at 300K



Fig. 23 Fracture modes of (a) a (40,0) zigzag nanotube with an initial crack of length 0.48 nm (Mode I fracture); (b) a (23,23) armchair nanotube with an initial crack of length 0.48nm (Mode I fracture); (c) a (23,23) armchair nanotube with an initial crack of length 0.92nm (Mixed Mode I/II fracture).



Mechanics of defected nanotubes (Nano-scale ~1nm)

- Vacancy defects are randomly located on nanotubes
- Reliability analysis of nanotubes is conducted
- Bending and torsion of nanotubes are also studied

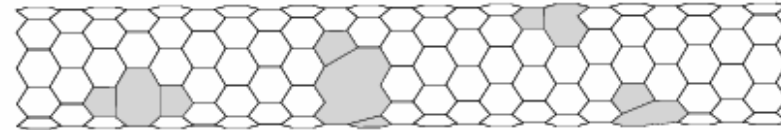


Fig. 24 Configuration of a (10,0) nanotube containing randomly located vacancy defects

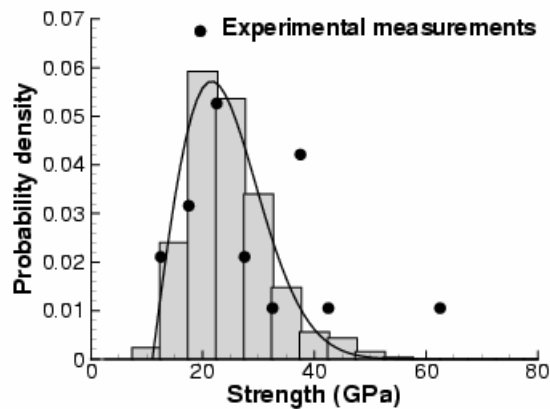


Fig. 25 Probability distribution of nanotube strength at the room temperature of 300K

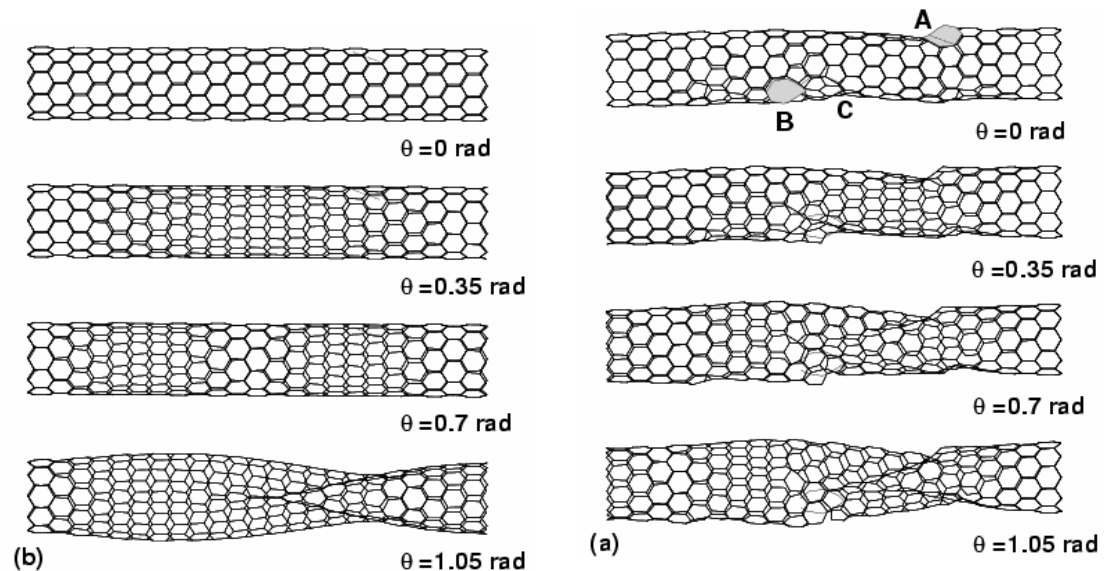


Fig. 26 The evolutions of the configuration of (a) a vacancy-defected (10,0) nanotube and (b) a pristine (10,0) nanotube

- Xiao and Hou, submitted to *Journal of Nanoscience and Nanotechnology*, 2007



Mechanics of nanotube reinforced composites (Nano-scale ~1nm)

- Embedded nanotubes are supposed to reinforce strength of composites
- Effects of the volume fraction of embedded nanotubes are significant
- Occurrence of defects weaken instead of reinforce nanocomposites

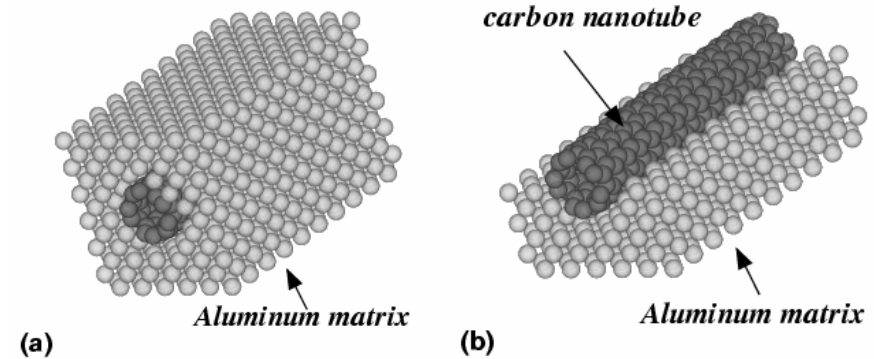


Fig. 27 Computational model of carbon nanotube/aluminum composites

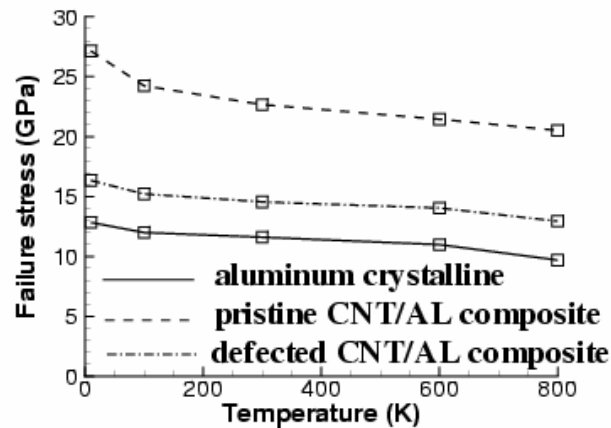


Fig. 28 Failure stresses of nanocomposites compared with those of aluminum crystalline

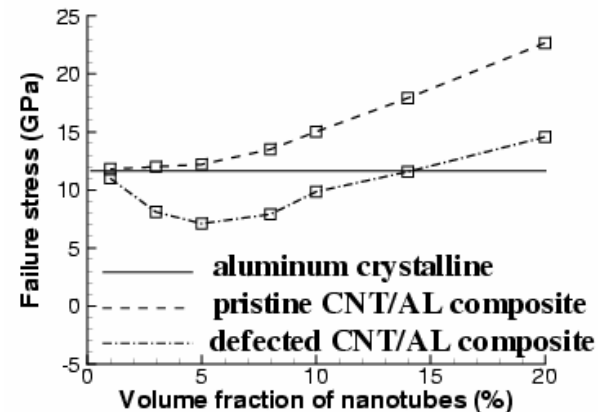


Fig. 29 Effects of volume fraction of embedded nanotubes on strength of CNT/Al composites

- Xiao and Hou, *Physical Review B*, Vol 73, 2006, 115406



Mechanics of nanotube reinforced composites (Nano-scale ~1nm)

- Multiscale modeling and simulation
- SWNT, MWNT, and SWNT bundles are considered

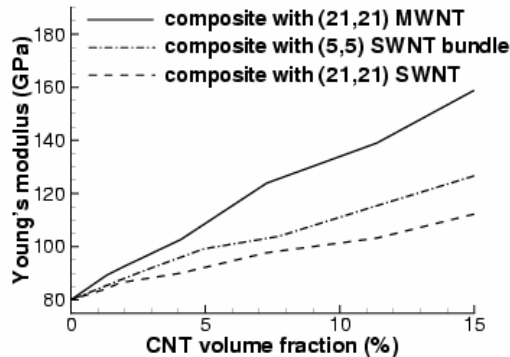


Fig. 31 Young's moduli of composites

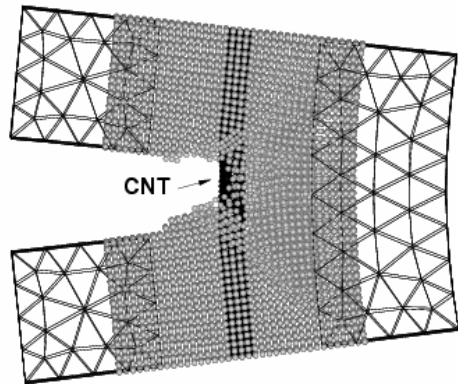


Fig. 32 CNT can resist crack propagation in composites

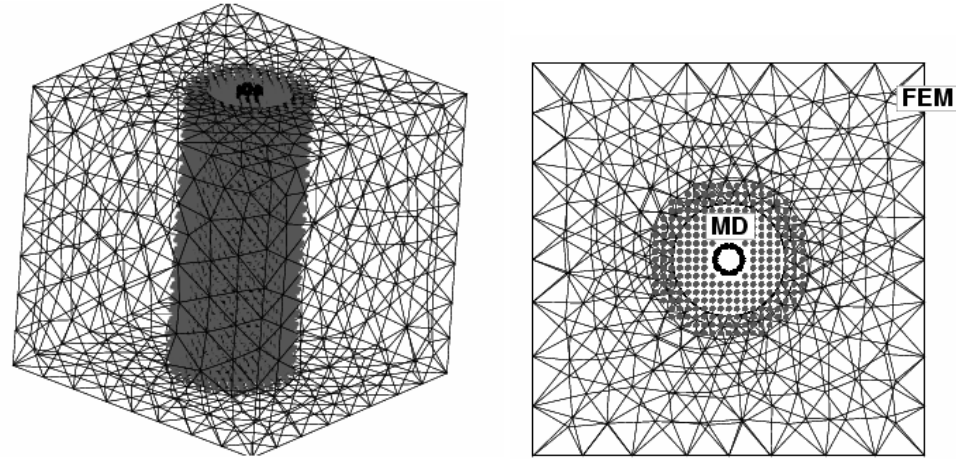


Fig. 30 multiscale model of CNT/Al composites

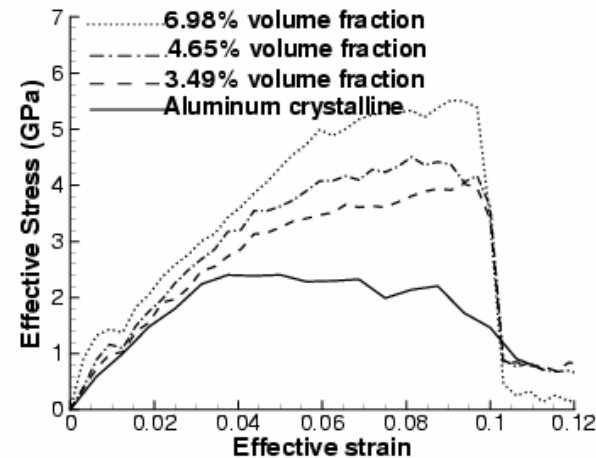


Fig. 33 stress-strain relations when materials subject to mode I fracture

- Xiao and Hou, *International Journal for Multiscale Computational Engineering*, submitted, 2007



Nanoelectromechanical systems (Nano-scale ~1nm)

- Nanotube-based oscillators can have high frequency
- They may stop at finite temperatures
- A NEMS design as memory cells is proposed

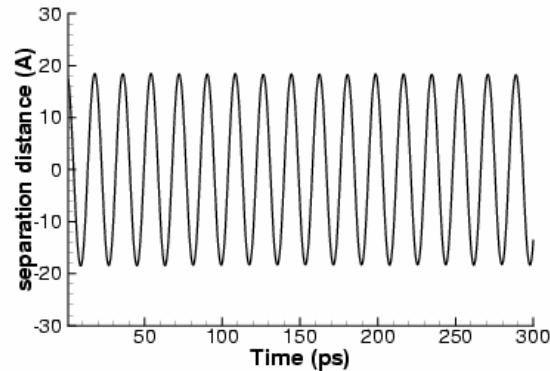
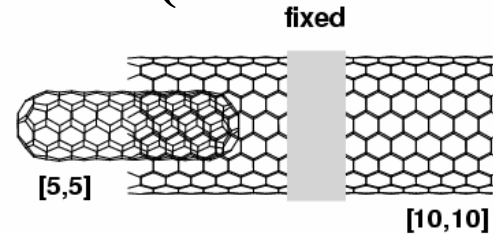


Fig. 34 A [5,5]/[10,10] nanotube-based oscillator can have a frequency of 55 GHz when it is isolated with a zero initial temperature

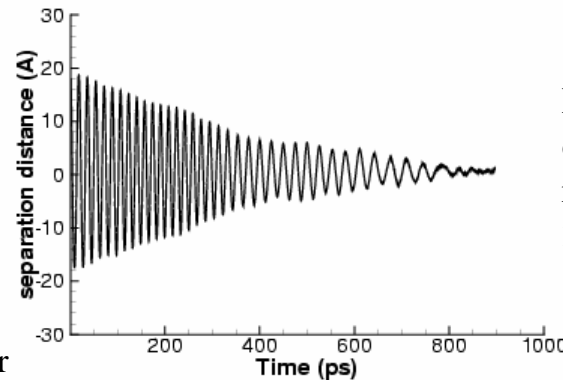


Fig. 35 The nano-oscillator stops at the room temperature of 300K

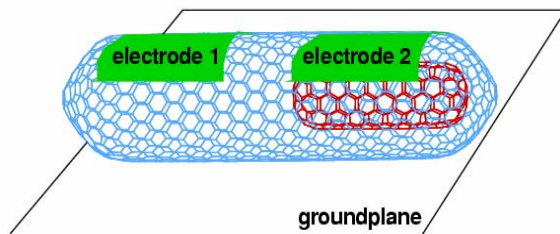
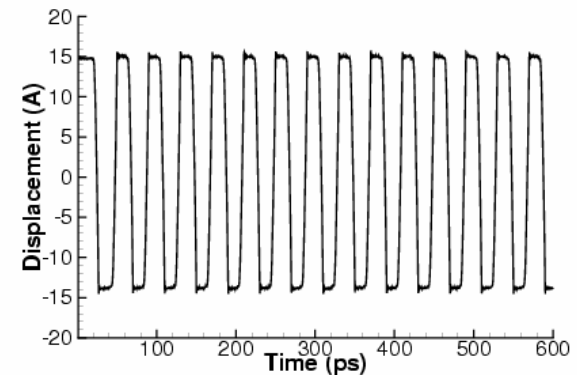


Fig. 36 A NEMS for memory cells (above). When a voltage pulse applied on electrodes, a stable oscillation can be observed (right). Such mechanism can be read as switchable logic 0/1 signals.



- Xiao et. al., *International Journal of Computational and Theoretical Nanoscience*, Vol. 3, 2006, pp 142-147
- Xiao et. al., *International Journal of Nanoscience*, Vol 5(1), 2006, pp 47-55



Nanotube-based resonant oscillator (Nano-scale ~1nm)

- Multiscale modeling and simulation of nanotube-based resonant oscillator
- Comparing well with experimental results
- Energy dissipation depending on the resonance frequency

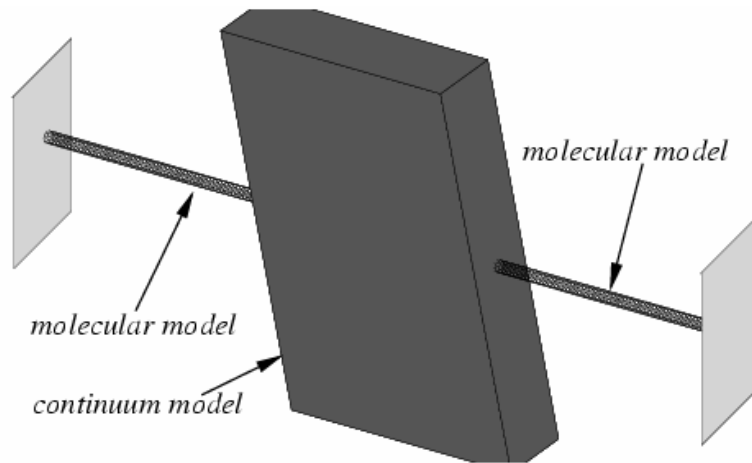


Fig. 37 Multiscale modeling of resonant oscillators

Fig. 39 Effects of resonance frequencies on energy dissipation (right)

- Xiao and Hou, *Nanoscale research letters*, Vol 2(1), 2007, 54-59
- Xiao and Hou, *Physical Review B*, Vol 75, 2007, 125414

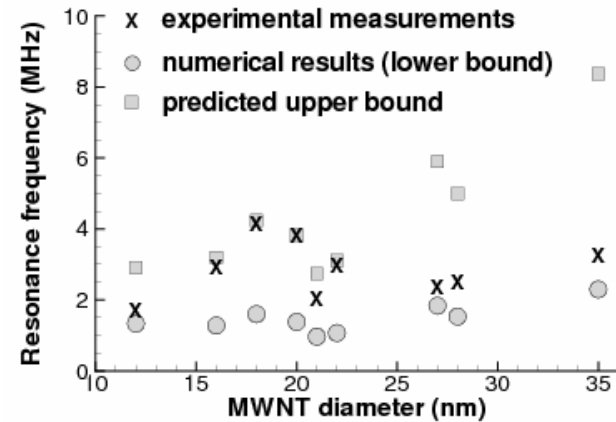


Fig. 38 Comparison with experiments (Papadakis et. al. 2004)

